Research Square

Preprints are preliminary reports that have not undergone peer review.
They should not be considered conclusive, used to inform clinical practice,
or referenced by the media as validated information.

Synthesis, characterization, crystal structures and urease inhibition of Cu^{II}, Co^{II} and Zn^{II} complexes derived from *N'*-(5-chloro-2-hydroxybenzylidene)-3-methylbenzohydrazide

Yang-Lei Li
Sichuan University of Arts and Science
Yao-Yao Cao
Jiangsu Ocean University
Jin Mu
Sichuan University of Arts and Science
Yu-Qun Ye
Sichuan University of Arts and Science
Da-Hua Shi
Jiangsu Ocean University
Yu-Qing Gu
Zhangwu Senior High School
Zhong-Lu You
youzhonglu@126.com

Sichuan University of Arts and Science

Research Article

Keywords: Copper complex, cobalt complex, zinc complex, hydrazone, urease inhibition

Posted Date: May 7th, 2026

DOI: https://doi.org/10.21203/rs.3.rs-9479406/v1

License: This work is licensed under a Creative Commons Attribution 4.0 International License.
Read Full License

Additional Declarations: No competing interests reported.

Version of Record: A version of this preprint was published at Transition Metal Chemistry on August 10th, 2026. See the published version at https://doi.org/10.1007/s11243-026-00768-5.

Abstract

Hydrazone compounds have a wide range of biological activities and play an important role in coordination chemistry. In this study, four new copper(II), cobalt(II) and zinc(II) complexes, $[Cu_2L_2(ONO_2)_2]$ (**1**), $[Co_2L_2(EtOH)_2(OH_2)_2](NO_3)_2$ (**2**), $[Co_2L_2(EtOH)_2(OH_2)_2]Cl_2$ (**3**) and $[ZnL_2]_n$ (**4**), where L is the deprotonated *N'*-(5-chloro-2-hydroxybenzylidene)-3-methylbenzohydrazide (HL), were prepared and structurally characterized. Molecular structures of the complexes were determined by single crystal X-ray diffraction. Complexes **1**, **2** and **3** are dinuclear structures, and complex **4** is a polymeric structure. The tridentate hydrazone ligands in the complexes chelate to the metal centers through imino N, phenolate and carbonyl O atoms. Inhibitory effect of the four complexes on *Jack bean* urease was assayed. As a result, the copper(II) complex exhibited the best inhibitory effect (IC_{50} = 1.1 ± 0.3 μmol L^{-1}), while the two cobalt(II) complexes showed moderate effects, and the zinc(II) complex had no activity.

Introduction

Urease (EC 3.5.1.5) is a nickel-dependent metalloenzyme responsible for hydrolyzing urea into carbon dioxide and ammonia. Urease is widely distributed in most organisms, including bacteria, fungi, algae, plants, and even animals and humans. In the presence of urease, urea decomposes into ammonia at a rate 10^{14} times faster than without urease. This process raises soil pH, which can damage plants by depriving them of essential nutrients [1, 2]. Excessive urease activity can also trigger many pathological processes, such as peptic ulcers, urinary catheter encrustation, kidney stones, pyelonephritis, urinary tract calculi, hepatic encephalopathy and arthritis in humans and animals [3, 4]. High level of urease can lead to agricultural economic and environmental safety issues, such as air and water pollution. Therefore, controlling the activity of urease is necessary. In the last few years, various urease inhibitors include phosphate esters, hydroxylamine derivatives, hydroxamic acids, polyphenols, imidazole derivatives and metal complexes have been reported [5–8]. However, most of the inhibitors have side effects or low efficiency, which limits their practical application [9, 10].

Hydrazone is a class of compounds with broad biological activity, which can act as an excellent ligand to coordinate with transition metal ions to form complexes with versatile structures [11–13]. Substances containing chlorine substituents have potential biological activity [14, 15]. Metal complexes derived from hydrazone ligands exhibit good physiological and pharmacological activities, some of which have shown urease inhibitory activity [16–18]. Our research group has focused on Schiff base complexes as urease inhibitors [19–21]. To construct new complexes containing chloro and methyl substituents in hydrazone ligands and explore novel urease inhibitors, this study presents four new copper(II), cobalt(II), and zinc(II) complexes derived from *N'*-(5-chloro-2-hydroxybenzylidene)-3-methylbenzohydrazide (HL; Scheme 1).

Experimental

Materials and measurements

5-Chloro-2-hydroxybenzaldehyde, 3-methylbenzohydrazide, and acetohydroxamic acid (analytical grade) were obtained from Macklin Biochemical Technology Co., Ltd. $Cu(NO_3)_2{\cdot}3H_2O$, $Co(NO_3)_2{\cdot}6H_2O$, $CoCl_2{\cdot}6H_2O$ and ZnI_2 were purchased from Liaodong Chemical Reagent Co., Ltd. Urea was supplied by Sigma-Aldrich Co. (St. Louis, USA). All other chemicals were of commercial grade and used as received. Elemental analysis (CHN) was performed on a Perkin-Elmer 240C elemental analyzer. Infrared (IR) spectra were recorded as KBr pellets using a Nicolet AVATAR 360 Fourier transform infrared spectrometer in the range of 4000 – 400 cm^{-1}. Ultraviolet-visible (UV-Vis) spectra were measured on a Lambda 35 UV-Vis spectrophotometer. The molar conductivity of the complexes was determined using a DDS-11A conductivity meter. ^1H and ^{13}C NMR spectra of H_2L were recorded on a Bruker 500 MHz NMR spectrometer. Single-crystal structures of the four complexes were determined using a Bruker Apex II CCD diffractometer.

Synthesis of HL

5-Chloro-2-hydroxybenzaldehyde (1.56 g, 0.010 mol) and 3-methylbenzohydrazide (1.50 g, 0.010 mol) were dissolved in absolute ethanol (50 mL). The mixture was stirred and refluxed for 25 min and then the solvent removed by distillation. The solid was re-crystallized from ethanol to give colorless crystalline product. Yield: 2.73 g (95%). $C_{15}H_{13}ClN_2O_2$: calcd.: C 62.40; H 4.54; N 9.70%; found: C 62.23; H 4.62; N 9.61%. Characteristic IR: $\bar{\upsilon}$ = 3207 ν(NH), 1646 ν(C = O), 1607 ν(C = N) cm^{-1}. UV-Vis data (λ_{max}, ε): 240 nm, 15,735 L mol^{-1} cm^{-1}; 287 nm, 19,930 L mol^{-1} cm^{-1}; 300 nm, 17,570 L mol^{-1} cm^{-1}; 339 nm, 10,752 L mol^{-1} cm^{-1}. ^1H NMR (500 MHz, DMSO-d_6): δ 12.13 (s, 1H, NH), 11.29 (s, 1H, OH), 8.62 (s, 1H, CH = N), 7.76 (s, 1H, ArH), 7.73 (t, 1H, ArH), 7.65 (d, 1H, ArH), 7.42 (d, 2H, ArH), 7.30 (d, 1H, ArH), 6.95 (d, 1H, ArH), 2.40 (s, 3H, CH_3). ^{13}C NMR (126 MHz, DMSO-d_6) δ 162.99, 155.99, 145.76, 137.83, 132.67, 132.55, 130.66, 128.37, 128.07, 127.60, 124.79, 122.92, 120.65, 118.17, 20.87.

Synthesis of the complexes

$[Cu_2L_2(ONO_2)_2]$ (1)

HL (0.10 mmol, 29 mg) was dissolved in ethanol (15 mL), to which was added dropwise a solution of $Cu(NO_3)_2{\cdot}3H_2O$ (0.10 mmol, 25 mg) in ethanol (15 mL) with stirring. The mixture was heated under reflux for 30 min, then cooled to room temperature to yield a clear green solution. The solution was left to stand for one week to obtain deep green crystals. Yield: 23 mg (56%). $C_{30}H_{24}Cl_2Cu_2N_6O_{10}$: calcd.: C 43.59; H 2.93; N 10.17%; found: C 43.41; H 3.02; N 10.25%. Characteristic IR: $\bar{\upsilon}$ = 3160 ν(N–H), 1617 ν(C = O), 1604 ν(C = N), 1300 ν(ONO_2) cm^{-1}. UV-Vis data (λ_{max}, ε): 230 nm, 23,320 L mol^{-1} cm^{-1}; 267 nm, 19,988 L mol^{-1} cm^{-1}; 314 nm, 13,992 L mol^{-1} cm^{-1}; 404 nm, 11,326 L mol^{-1} cm^{-1}.

[CoL(EtOH)(OH)](NO) (2)

HL (0.10 mmol, 29 mg) was dissolved in ethanol (15 mL), to which was added dropwise a solution of $Co(NO_3)_2{\cdot}6H_2O$ (0.10 mmol, 29 mg) in ethanol (15 mL) with stirring. The mixture was heated under reflux for 30 min under argon atmosphere, then cooled to room temperature to yield a clear pink solution. The solution was left to stand for one week under nitrogen atmosphere to obtain pink crystals. Yield: 29 mg (62%). $C_{34}H_{40}Cl_2Co_2N_6O_{14}$: calcd.: C 43.19; H 4.26; N 8.89%; found: C 43.03; H 4.15; N 8.96%. Characteristic IR: $\bar{\upsilon}$ = 3503 ν(O–H), 3220 ν(N–H), 1618 ν(C = O), 1601 ν(C = N), 1385 ν(NO_3) cm^{-1}. UV-Vis data (λ_{max}, ε): 230 nm, 23,320 L mol^{-1} cm^{-1}; 267 nm, 19,988 L mol^{-1} cm^{-1}; 314 nm, 13,992 L mol^{-1} cm^{-1}; 404 nm, 11,326 L mol^{-1} cm^{-1}.

$[Co_2L_2(EtOH)_2(OH_2)_2]Cl_2$ (3)

The preparation method of this complex is similar to that of complex **2**, with $Co(NO_3)_2{\cdot}6H_2O$ replaced by $CoCl_2{\cdot}6H_2O$ (0.10 mmol, 24 mg). Pink single crystals were obtained. Yield: 26 mg (58%). $C_{34}H_{40}Cl_4Co_2N_4O_8$: calcd.: C 45.76; H 4.52; N 6.28%; found: C 45.53; H 4.60; N 6.17%. Characteristic IR: $\bar{\upsilon}$ = 3425 ν(O–H), 3143 ν(N–H), 1617 ν(C = O), 1601 ν(C = N) cm^{-1}. UV-Vis data (λ_{max}, ε): 235 nm, 22,160 L mol^{-1} cm^{-1}; 268 nm, 21,760 L mol^{-1} cm^{-1}; 300 nm, 15,832 L mol^{-1} cm^{-1}; 340 nm, 10,280; 420 nm, 5,020 L mol^{-1} cm^{-1}.

[ZnL] (4)

The preparation method of this complex is similar to that of complex **1**, with $Cu(NO_3)_2{\cdot}3H_2O$ replaced by ZnI_2 (0.10 mmol, 32 mg). Colorless single crystals were obtained. Yield: 45 mg (70%). $C_{30}H_{24}Cl_2N_4O_4Zn$: calcd.: C 56.23; H 3.77; N 8.74%; found: C 56.41; H 3.72; N 8.63%. Characteristic IR: $\bar{\upsilon}$ = 3439 ν(N–H), 1621 ν(C = O), 1606 ν(C = N) cm^{-1}. UV-Vis data (λ_{max}, ε): 265 nm, 13,720 L mol^{-1} cm^{-1}; 288 nm, 23,100 L mol^{-1} cm^{-1}; 300 nm, 24,245 L mol^{-1} cm^{-1}; 340 nm, 9,710; 400 nm, 9,135 L mol^{-1} cm^{-1}.

Crystal structure determination

Single crystals suitable for X-ray diffraction were selected and mounted on the diffractometer equipped with a fine-focus sealed tube graphite monochromator, and Mo Kα radiation (λ = 0.71073 Å). Collected data were corrected for Lorentz-polarization effects and linear absorption. Multi-scan absorption correction based on ω scans was applied. Data refinement and data reduction were performed with SMART and SAINT software, respectively [22]. Structures of the four complexes were solved by the direct method with SHELXL and refined with anisotropic parameters [23]. All non-hydrogen atoms were anisotropically refined. Hydrogen atoms bonded to oxygen in ethanol and water molecules, as well as those bonded to nitrogen in the hydrazone ligands, were located from difference Fourier maps and refined isotropically. O–H, N–H, and H···H bond lengths were constrained to 0.85(1), 0.90(1), and 1.37(2) Å, respectively. All other hydrogen atoms were geometrically fixed and refined using the riding model. All

calculations were performed with the SHELXL software. A summary of crystallographic data and structural refinement parameters is presented in Table 1.

Table 1
Crystallographic and experimental data for the complexes

Compound	**1**	**2**	**3**	**4**
Formula	$C_{30}H_{24}Cl_2Cu_2N_6O_{10}$	$C_{34}H_{40}Cl_2Co_2N_6O_{14}$	$C_{34}H_{40}Cl_4Co_2N_4O_8$	$C_{30}H_{24}Cl_2N_4O_4Zn$
Formula Weight	826.53	945.48	892.36	640.80
Crystal shape/color	Block/green	Block/pink	Block/pink	Block/colorless
Crystal size/mm^3	0.11·0.09·0.08	0.32·0.28·0.26	0.19·0.18·0.15	0.21·0.18·0.17
Crystal system	Triclinic	Triclinic	Triclinic	Monoclinic
Space group	*P*-1	*P*-1	*P*-1	$P2_1/c$
a /Å	7.7760(2)	8.8905(13)	8.6759(15)	12.5851(8)
b /Å	14.7060(3)	10.7839(17)	9.4913(16)	6.0921(4)
c /Å	15.4029(3)	12.5759(17)	13.7036(18)	18.6894(12)
α /º	108.027(1)	113.270(2)	106.407(2)	90
β /º	97.448(1)	92.185(2)	106.110(2)	96.546(1)
γ /º	104.118(1)	107.408(2)	96.019(2)	90
V /$Å^3$	1583.64(6)	1040.0(3)	1019.2(3)	1423.57(16)
Z	2	1	1	2
D_c /(g/cm^{-3})	1.733	1.510	1.454	1.495
μ /mm^{-1}	1.581	0.997	1.127	1.094
F(000)	836	486	458	656
θ range/º	2.43–25.50	2.16–25.50	2.28–25.50	2.19–25.50
Reflections	17512	9672	9410	14716
Unique reflections	5889	3854	3740	2652
Observed reflections ($I \geq 2\sigma(I)$)	4354	1711	1936	2360

Compound	1	2	3	4
Parameters	458	275	249	190
Restraints	2	5	5	1
Goodness-of-fit on F^2	1.023	0.951	0.953	1.034
R_1, wR_2 [$I \geq 2\sigma(I)$]	0.0338, 0.0729	0.0773, 0.1648	0.0701, 0.1526	0.0341, 0.0802
R_1, wR_2 (all data)	0.0570, 0.0817	0.1811, 0.2135	0.1474, 0.1846	0.0396, 0.0841

Urease inhibitory activity assay

The determination of urease inhibition was carried out by the literature method [24]. A mixture of 75 μL *Jack bean* urease and 75 μL of the test compound solution at different concentrations was pre-incubated for 15 minutes in a 96-well reaction plate. Acetohydroxamic acid (AHA) was used as the reference. Subsequently, 75 μL of pH 6.8 phosphate buffer (containing 0.18 mmol L^{-1} phenol red and 400 mmol L^{-1} urea) was added, and the mixture was incubated at room temperature. The time required for sufficient ammonium carbonate to form, causing the pH of the phosphate buffer to rise from 6.8 to 7.7, was determined using a microplate reader at 560 nm. The endpoint was determined by the color change of the phenol red indicator.

Results and discussion

Chemistry

The four metal complexes were facile synthesized according to Scheme 1. The copper(II) complex (**1**) was prepared by the reaction of HL with copper(II) nitrate in ethanol. The cobalt(II) complexes (**2**, **3**) were respectively obtained by the reaction of HL with cobalt(II) nitrate and cobalt(II) chloride in ethanol under an argon atmosphere. The zinc(II) complex (**4**) was synthesized by the reaction of HL with zinc iodide in ethanol. Crystals of the four complexes are stable for at least two weeks in air at room temperature. The complexes are soluble in *N,N*-dimethylformamide, dimethyl sulfoxide, methanol, ethanol, and acetonitrile, but insoluble in water. The elemental analysis results of the complexes are consistent with the chemical formulae given by single-crystal X-ray determination. In a 10^{-3} mol L^{-1} mixture of dimethyl sulfoxide and water (volume ratio 1:99), complexes **1** and **4** behave as non-electrolytes with molar conductivities of 43 and 27 Ω^{-1} cm² mol^{-1}, respectively; complexes **2** and **3** behave as 1:2 type electrolytes with molar conductivities of 213 and 220 Ω^{-1} cm² mol^{-1} [25].

Structure description of the complexes

$[Cu_2L_2(ONO_2)_2]$ (1)

A perspective view of this complex is shown in Fig. 1. The selected bond lengths and bond angles are listed in Table 2. The complex has a dinuclear copper(II) structure with a Cu···Cu separation of 2.914(2) Å. The two Cu atoms are bridged by two phenolate oxygen atoms, O1 and O3. The deprotonated hydrazone ligand chelates the Cu atoms through a phenolate oxygen atom (O1), an imine nitrogen atom (N1), and a carbonyl oxygen atom (O2). The Cu1 atom is in a square pyramidal geometry, with its basal plane defined by three coordinating atoms of the hydrazone ligand, and another oxygen atom (O3) from the other hydrazone ligand lying on the basal plane. The apical position is occupied by an oxygen atom (O8) from a nitrate ligand. The coordination mode of Cu2 is similar to that of Cu1. The square pyramidal coordination deviates from the ideal geometry, which can be observed from the bond distances and bond angles. The Cu–O and Cu–N bond lengths are comparable to those observed in copper(II) complexes containing hydrazone ligands [26, 27]. In the basal plane of the square pyramidal coordination, the *cis* and *trans* bond angle ranges for Cu1 are 80.79(8)º–104.49(8)º and 164.70(9)º–170.93(8)º, respectively, while those for Cu2 are 79.93(8)º–103.85(8)º and 167.64(9)º–169.03(9)º. The five-membered chelate rings Cu1–N1–N2–C8–O2, Cu2–N3–N4–C23–O4, and the four-membered chelate ring Cu1–O1–Cu2–O3 collectively lead to the distortion. The two benzene rings of the hydrazone ligand form dihedral angles of 3.8(3)º and 11.8(3)º, respectively.

Table 2
Selected bond lengths/Å and angles/° for the complexes

1			
Cu1–O1	1.9233(18)	Cu1–N1	1.929(2)
Cu1–O2	1.9564(19)	Cu1–O3	1.9571(18)
Cu1–O8	2.272(2)	Cu2–O3	1.9300(18)
Cu2–N3	1.936(2)	Cu2–O4	1.9433(19)
Cu2–O1	1.9848(18)	Cu2–O5	2.370(2)
O1–Cu1–N1	91.77(8)	O1–Cu1–O2	170.93(8)
N1–Cu1–O2	81.33(8)	O1–Cu1–O3	80.79(8)
N1–Cu1–O3	164.70(9)	O2–Cu1–O3	104.49(8)
O1–Cu1–O8	92.37(9)	N1–Cu1–O8	92.05(9)
O2–Cu1–O8	93.74(9)	O3–Cu1–O8	101.54(8)
O3–Cu2–N3	92.63(9)	O3–Cu2–O4	169.03(9)
N3–Cu2–O4	81.76(9)	O3–Cu2–O1	79.93(8)
N3–Cu2–O1	167.64(9)	O4–Cu2–O1	103.85(8)
O3–Cu2–O5	102.73(8)	N3–Cu2–O5	108.11(9)
O4–Cu2–O5	88.01(8)	O1–Cu2–O5	83.30(8)
2			
Co1–O1	2.017(4)	Co1–N1	2.035(6)
Co1–O1A	2.079(4)	Co1–O4	2.084(6)
Co1–O2	2.129(4)	Co1–O3	2.132(7)
O1–Co1–N1	88.2(2)	O1–Co1–O1A	80.7(2)
N1–Co1–O1A	168.75(19)	O1–Co1–O4	97.4(2)
N1–Co1–O4	95.4(2)	O1A–Co1–O4	87.8(2)
O1–Co1–O2	164.84(18)	N1–Co1–O2	76.8(2)
O1A–Co1–O2	114.26(19)	O4–Co1–O2	86.28(19)
O1–Co1–O3	90.6(2)	N1–Co1–O3	89.9(2)
Symmetry codes: A: 1 − *x*, 2 − *y*, 1 − *z*; B: *x*, 1 + *y*, *z*; C: 1 − *x*, 1 − *y*, 1 − *z*			

1			
O1A–Co1–O3	88.5(2)	O4–Co1–O3	170.6(2)
O2–Co1–O3	87.3(2)		
Symmetry code for A: 1 – *x*, – *y*, 1 – *z*			
3			
Co1–O1	2.054(4)	Co1–N1	2.079(5)
Co1–O3	2.099(5)	Co1–O1A	2.137(4)
Co1–O2	2.151(4)	Co1–O4	2.185(5)
O1–Co1–N1	89.01(17)	O1–Co1–O3	96.9(2)
N1–Co1–O3	92.3(2)	O1–Co1–O1A	80.92(17)
N1–Co1–O1A	169.62(17)	O3–Co1–O1A	86.43(18)
O1–Co1–O2	165.15(17)	N1–Co1–O2	76.87(18)
O3–Co1–O2	88.4(2)	O1A–Co1–O2	113.36(16)
O1–Co1–O4	92.78(17)	N1–Co1–O4	90.18(19)
O3–Co1–O4	170.1(2)	O1A–Co1–O4	92.80(17)
O2–Co1–O4	82.81(18)		
Symmetry code for A: 1 – *x*, 2 – *y*, 1 – *z*			
4			
Zn1–N1	2.0420(16)	Zn1–N1A	2.0420(16)
Zn1–O1	2.0421(14)	Zn1–O1A	2.0421(14)
Zn1–O2B	2.3321(15)	Zn1–O2C	2.3321(15)
N1–Zn1–N1A	180	N1–Zn1–O1	78.94(6)
N1A–Zn1–O1	101.06(6)	N1–Zn1–O1A	101.06(6)
O1–Zn1–O1A	180	N1–Zn1–O2B	92.33(6)
N1A–Zn1–O2	87.67(6)	O1–Zn1–O2B	93.13(6)
O1A–Zn1–O2B	86.86(6)	N1–Zn1–O2C	87.67(6)
N1A–Zn1–O2C	92.33(6)	O1–Zn1–O2C	86.87(6)
O1A–Zn1–O2C	93.14(6)	O2B–Zn1–O2C	180
Symmetry codes: A: 1 – *x*, 2 – *y*, 1 – *z*; B: *x*, 1 + *y*, *z*; C: 1 – *x*, 1 – *y*, 1 – *z*			

In the crystal structure, the complex molecules are connected by intermolecular N–H···O hydrogen bonds (Table 3), forming one-dimensional chains extending along the *b*-axis (Fig. 2).

Table 3
Hydrogen bond distances (Å) and angles (º) for the complexes

D*–H•••*A	***d*(*D*–H)**	***d*(H•••*A*)**	***d*(*D*•••*A*)**	**Angle (*D*–H•••*A*)**
1				
N4–H4•••O9^{i}	0.90(1)	2.04(1)	2.921(3)	165(4)
N2–H2•••O5^{ii}	0.90(1)	1.86(2)	2.723(3)	162(4)
2				
N2–H2•••O6^{iii}	0.90(1)	2.00(2)	2.899(8)	174(8)
O4–H4B•••N3^{iv}	0.85(1)	2.63(3)	3.444(8)	161(8)
O4–H4B•••O7^{iv}	0.85(1)	2.07(3)	2.886(7)	160(6)
O4–H4B•••O6^{iv}	0.85(1)	2.52(6)	3.190(7)	136(7)
O4–H4A•••O7^{iii}	0.85(1)	2.08(4)	2.844(8)	150(7)
O3–H3•••O5	0.85(1)	1.93(4)	2.742(8)	159(10)
3				
O4–H4•••Cl1^{ii}	0.85(1)	2.33(1)	3.182(5)	177(7)
O3–H3A•••Cl1^{v}	0.85(1)	2.40(2)	3.232(5)	167(7)
O3–H3B•••Cl1^{vi}	0.85(1)	2.33(1)	3.169(5)	172(6)
N2–H2•••Cl1	0.90(1)	2.46(2)	3.339(6)	167(6)
4				
N2–H2•••O2	0.90(1)	1.63(1)	2.516(2)	166(4)
Symmetry codes: i) 1 − *x*, 2 − *y*, 1 − *z*; ii) 1 − *x*, 1 − *y*, 1 − *z*; iii) 1 − *x*, − *y*, 1 − *z*; iv) 1 + *x*, *y*, *z*; v) *x*, 1 + *y*, *z*; vi) − *x*, 1 − *y*, 1 − *z*.				

$[Co_2L_2(EtOH)_2(OH_2)_2](NO_3)_2$ (2) and $[Co_2L_2(EtOH)_2(OH_2)_2]Cl_2$ (3)

Perspective views of these complexes are shown in Figs. 3 and 4. Selected bond distances and bond angles are listed in Table 2. Complex **2** contains a dinuclear $[Co_2L_2(EtOH)_2(OH_2)_2]$ cation and two nitrate

anions. Similarly, complex **3** contains a dinuclear $[Co_2L_2(EtOH)_2(OH_2)_2]$ cation and two chloride anions. Thus, the cationic structures of both complexes are identical. The deprotonated hydrazone ligand coordinates to cobalt atoms through phenoxide oxygen (O1), imine nitrogen (N1), and carbonyl oxygen (O2) atoms. The cobalt atoms are octahedrally coordinated, with the equatorial plane consisting of three coordinating atoms from the hydrazone ligand and one oxygen atom from another hydrazone ligand (O1A; symmetry code A: 1 – *x*, 2 – *y*, 1 – *z*). The axial positions are occupied by two oxygen atoms from ethanol and water ligands (O3 and O4). The octahedral coordination deviates from the ideal geometry, which can be observed from the bond distances and bond angles. The Co–O and Co–N bond distances in the cations of the two complexes are comparable to each other, and comparable to those observed in cobalt(II) complexes containing hydrazone ligands [28, 29]. The ranges of *cis* and *trans* bond angles for the octahedral coordination are 76.8(2)°–114.3(2)° and 164.8(2)°–170.6(2)° for **2**, and 76.9(2)°–113.4(2)° and 165.2(2)°–170.1(2)° for **3**, respectively. The five-membered chelate ring Co1–N1–N2–C8–O2 and the four-membered chelate ring Co1–O1–Co1A–O1A lead to the distortion. The dihedral angles formed by the two benzene rings of the hydrazone ligand are 12.5(7)° for **2** and 4.4(6)° for **3**.

In the crystal structure of **2**, the cations are linked *via* hydrogen bonds (Table 3) through nitrate anions, forming one-dimensional chains extending along the *a*-axis (Fig. 5). In the crystal structure of **3**, the cations are linked *via* hydrogen bonds (Table 3) through chloride ions, forming a two-dimensional network parallel to the *ab* plane (Fig. 6).

$[ZnL_2]_n$ (4)

The perspective view of this complex is shown in Fig. 7. The selected bond distances and bond angles are listed in Table 2. The complex adopts a polymeric structure, with the smallest repeating unit containing a $[ZnL_2]$ fragment. The deprotonated hydrazone ligand coordinates to the Zn atom through phenolate oxygen (O2), imine nitrogen (N1), and carbonyl oxygen (O1) atoms. The Zn atom is in an octahedral coordination environment, with the equatorial plane consisting of two imine nitrogens (N1, N1A; symmetry code for A: 1 – *x*, 2 – *y*, 1 – *z*) and two carbonyl oxygens (O1, O1A) from two hydrazone ligands. The axial positions are occupied by two phenolate oxygens (O2B, O2C; symmetry codes: B: *x*, 1 + *y*, *z*; C: 1 – *x*, 1 – *y*, 1 – *z*) from two symmetry-related hydrazone ligands. The octahedral coordination deviates from the ideal geometry, which can be observed from the bond lengths and bond angles. The Zn–O and Zn–N bond lengths are comparable to those observed in zinc(II) hydrazone complexes [30, 31]. The *cis* and *trans* bond angles in the octahedral coordination range from 78.94(6)° to 101.06(6)° and 180°, respectively. The five-membered chelate ring Zn1–N1–N2–C8–O1 causes coordination distortion. The two benzene rings of the hydrazone ligand form a dihedral angle of 9.3(2)°.

In the crystal structure of the complex, $[CuL_2]$ units are bridged by phenolate and carbonyl oxygen atoms to form one-dimensional chains extending along the *b*-axis (Fig. 8).

IR and UV-Vis spectra

In the infrared spectrum of HL, the characteristic absorption bands at 1646 cm^{-1} and 1607 cm^{-1} are assigned to v(C = O) and v(C = N), respectively [32]. In the spectra of the four complexes, the stretching vibration frequencies of the C = N group are lower than that of HL, ranging from 1601–1606 cm^{-1}, indicating that the hydrazone ligand coordinates with the metal atoms through the imine nitrogen. The characteristic strong absorption band of the nitrate ligand in complex **1** appears at 1300 cm^{-1}, while the strong absorption band of the nitrate anion in complex **2** is observed at 1385 cm^{-1} [33]. In the electronic spectra of the complexes, the absorption in the 230–270 nm range is attributed to π-π* transitions, and the absorption near 300–315 nm is assigned to n-π* transitions. The absorption band in the 400–420 nm range can be ascribed to ligand-to-metal charge transfer [34].

Urease inhibitory activity

Table 4 summarizes the inhibitory activity of *Jack bean* urease. The free hydrazone (HL) exhibited weak inhibitory activity against urease. The copper(II) and cobalt(II) complexes (**1**, **2** and **3**) showed higher activity, while the zinc complex (**4**) had lower activity than HL. Among them, the copper complex exhibited the strongest activity (IC_{50} = 1.1 ± 0.3 μmol L^{-1}), which was superior to copper nitrate and AHA. The two cobalt complexes showed moderate activity (41–43%) at a concentration of 100 μmol L^{-1}; their activity was also higher than that of cobalt nitrate but lower than that of AHA. The zinc complex had the lowest activity, even lower than zinc iodide. The copper complexes in this study showed better urease inhibitory activity than copper(II) complexes with Schiff base ligands such as *N,N′*-bis(4-fluorosalicylideneimino)-1,2-diaminopropane (IC_{50} = 2.1–3.4 μmol L^{-1}) [35], reduced Schiff base ligand 2,2'-((propane-1,3-diylbis(azanediyl))bis(methylene))diphenol (IC_{50} = 1.6 μmol L^{-1}) [36], and Schiff base ligands derived from tyrosine and 3,5-dibromosalicylaldehyde, 5-chlorosalicylaldehyde, or 2-hydroxy-1-naphthaldehyde (IC_{50} = 2.15–32.12 μmol L^{-1}) [37]. Therefore, the copper complexes in this study can be considered as a novel urease inhibitor.

Table 4
Urease inhibition of the compounds

Tested materials	Percentage Inhibition[a]	IC_{50}(μmol L^{-1})
HL	25 ± 1.6	–
1	98 ± 2.1	1.1 ± 0.3
2	41 ± 2.3	–
3	43 ± 3.0	–
4	5.2 ± 1.4	–
$Cu(NO_3)_2$	92 ± 2.1	5.6 ± 0.8
$Co(NO_3)_2$	33 ± 1.9	–
ZnI_2	15 ± 1.0	–
Acetohydroxamic acid	85 ± 2.6	23 ± 1.4

[a] The concentration is 100 μmol L^{-1}. – means no activity or IC_{50} > 100 μmol L^{-1}.

Conclusion

In summary, four new copper(II), cobalt(II), and zinc(II) complexes derived from the hydazone ligand *N'*-(5-chloro-2-hydroxybenzylidene)-3-methylbenzohydrazide have been prepared and characterized. The copper(II) complex adopts a dinuclear structure with copper atoms in a square pyramidal coordination environment. The cobalt(II) complexes also have dinuclear structures, with cobalt atoms coordinated in an octahedral geometry. The zinc(II) complex forms a polymeric structure, where zinc atoms are octahedrally coordinated. Among these, the copper complex exhibits the highest activity against *Jack bean* urease and may serve as a novel urease inhibitor.

Declarations

Funding:

This project was supported by the Talents of High-Level Scientific Research Fund of Sichuan University of Arts and Science (Project No. 2025GCC27XZ).

Data availability statement: The authors confirm that the data supporting the findings of this study are available within the article.

Author Contribution

Zhong-Lu You. Conception, supervision, writing. Yang-Lei Li. Writing the main manuscript. Yao-Yao Cao and Da-Hua Shi. Biological test. Jin Mu and Yu-Qun Ye. Chemical synthesis and characterization. Yu-Qing Gu. Chemical synthesis, Single crystal structure determination.

References

1. Ni WW, Fang HL, Ye YX, Li WY, Yuan CP, Li DD, Mao SJ, Li SE, Zhu QH, Ouyang H, Xiao ZP, Zhu HL (2020) Future Med Chem 12:1633
2. Ni WW, Liu Q, Ren SZ, Li WY, Yi LL, Jing H, Sheng LX, Wan Q, Zhong PF, Fang HL, Ouyang H, Xiao ZP, Zhu HL (2018) Bioorg Med Chem 26:4145
3. Montecucco C, Rappuoli R (2001) Nat Rev Mol Cell Biol 2:457
4. Mobley HLT, Hausinger RP (1989) Microbiol Rev 53:85
5. Song XY, Zhang WK, Bai Y, Zhang LL, Hu JC, Wu ZJ, Pan HQ (2026) J Agri Food Chem 74:9933
6. de Fatima A, Pereira CD, Olimpio CRSDG, Oliveira BGD, Franco LL, da Silva PHC (2018) J Adv Res 13:113
7. Babaei D, Moghadam ES, Navidpour L, Amini M (2025) J Agr Food Chem 73:3795
8. Kafarski P, Talma M (2018) J Adv Res 13:101
9. Xiao ZP, Shi WK, Wang PF, Wei W, Zeng XT, Zhang JR, Zhu N, Peng M, Peng B, Lin XY, Ouyang H, Peng XC, Wang GC, Zhu HL (2015) Bioorg Med Chem 23:4508
10. Xiao ZP, Peng ZY, Dong JJ, He J, Ouyang H, Peng YT, Lu CL, Lin WQ, Wang JX, Xiang YP, Zhu HL (2013) Eur J Med Chem 63:685
11. Savic M, Pevec A, Novakovic I, Matic IZ, Stanojkovic T, Zlatar M, Gruden M, Turel I, Cobeljic B (2025) J Coord Chem 78:2357
12. Kargar H, Fallah-Mehrjardi M, Munawar KS (2024) Coord Chem Rev 501:215587
13. Fallah-Mehrjardi M, Kargar H, Munawar KS (2024) Inorg Chim Acta 560:121835
14. Kaleem S, Ullah H, Nabi M, Hussain R, Khan S, Sajid M, Iqbal N, Rahim F, Iqbal T, Hussain A, Iqbal R, Zahid Z, Mohany M, Aghayeva S (2024) Res Chem 8:101603
15. Alzahrani AYA, Ullah H, Rahim F, Alraih AM, Khan S, Hussain A, Hussain R, Iqbal N, Nawaz F (2024) J Mol Struct 1316:138908
16. Asadi M, Sayahi MH, Talebi M, Dastyafteh N, Esmkhani M, Mohammadi-Khanaposhtani M, Hosseini A, Amanlou M, Azizian H, Mahdavi M, Naz F, Khan KM (2025) J Mol Struct 1339:142307
17. Ahmad S, Khan M, Shah MIA, Ali M, Alam A, Riaz M, Khan KM (2022) ACS Omega 7:45077
18. Wang CF, Chen ZJ, Zhao KD, Chen XF, Zhang CY, Sheng GH, Zhu HL (2016) J Coord Chem 69:2656
19. You ZL, Yu HY, Zheng BY, Zhang CL, Lv CW, Li K, Pan L (2018) Inorg Chim Acta 469:44
20. He BH, Wang QY, Zhang XQ, Shi DH, You ZL (2023) Inorg Chim Acta 558:121738
21. Wang QY, He BH, Zhang XQ, Cao Y, Li A, Wang JQ, Shi DH, You ZL (2023) J Coord Chem 76:1604
22. Bruker SMART (2002) and SAINT Bruker AXS Inc., Madison

23. Sheldrick GM (2008) Acta Crystallogr A64:112
24. Meletiadis J, Meis JFGM, Mouton JW, Donnelly JP, Verweij PE (2000) J Clin Microbiol 38:2949
25. Geary WJ (1971) Coord Chem Rev 7:81
26. Xu GH, Tang BB, Gu L, Zhou P, Li H (2016) J Mol Struct 1120:205
27. Lago AB, Pino-Cuevas A, Carballo R, Vazquez-Lopez EM (2021) CrystEngComm 23:153
28. Wu LM, Teng HB, Feng XC, Ke XB, Zhu QF, Su JT, Xu WJ, Hu XM (2007) Cryst Growth Des 7:1337
29. Vrdoljak V, Pavlovic G, Hrenar T, Rubcic M, Siega P, Dreos R, Cindric M (2015) RSC Adv 5:104870
30. Xu GH, Tang BB, Hao L, Liu GL, Li H (2017) CrystEngComm 19:781
31. Wang JF, Liu B, Liu XM, Panzner MJ, Wesdemiotis C, Pang Y (2014) Dalton Trans 43:14142
32. Saheb V, Sheikhshoaie I, Setoodeh N, Rudbari HA, Bruno G (2013) Spectochim Acta A –. Mol Biomol Spectrosc 110:124
33. Chandra S, Sharma AK (2009) J Coord Chem 62:3688
34. You Z, Qiao Z, Cao Y, Shi D, Song N, Feng X (2025) Acta Chim Slov 72:740
35. Luo Y, Wang J, Zhang B, Guan Y, Yang T, Li X, Xu L, Wang J, You Z (2020) J Coord Chem 73:1765
36. Duan MM, Li YM, Xu LY, Yang HL, Luo FW, Guan YX, Zhang BT, Jing CL, You ZL (2019) Inorg Chem Commun 100:27
37. Wang H, Xu C, Zhang X, Zhang D, Jin F, Fan Y (2020) J Inorg Biochem 204:110959

Schemes

Schemes 1 and 2 are available in the Supplementary Files section

Figures

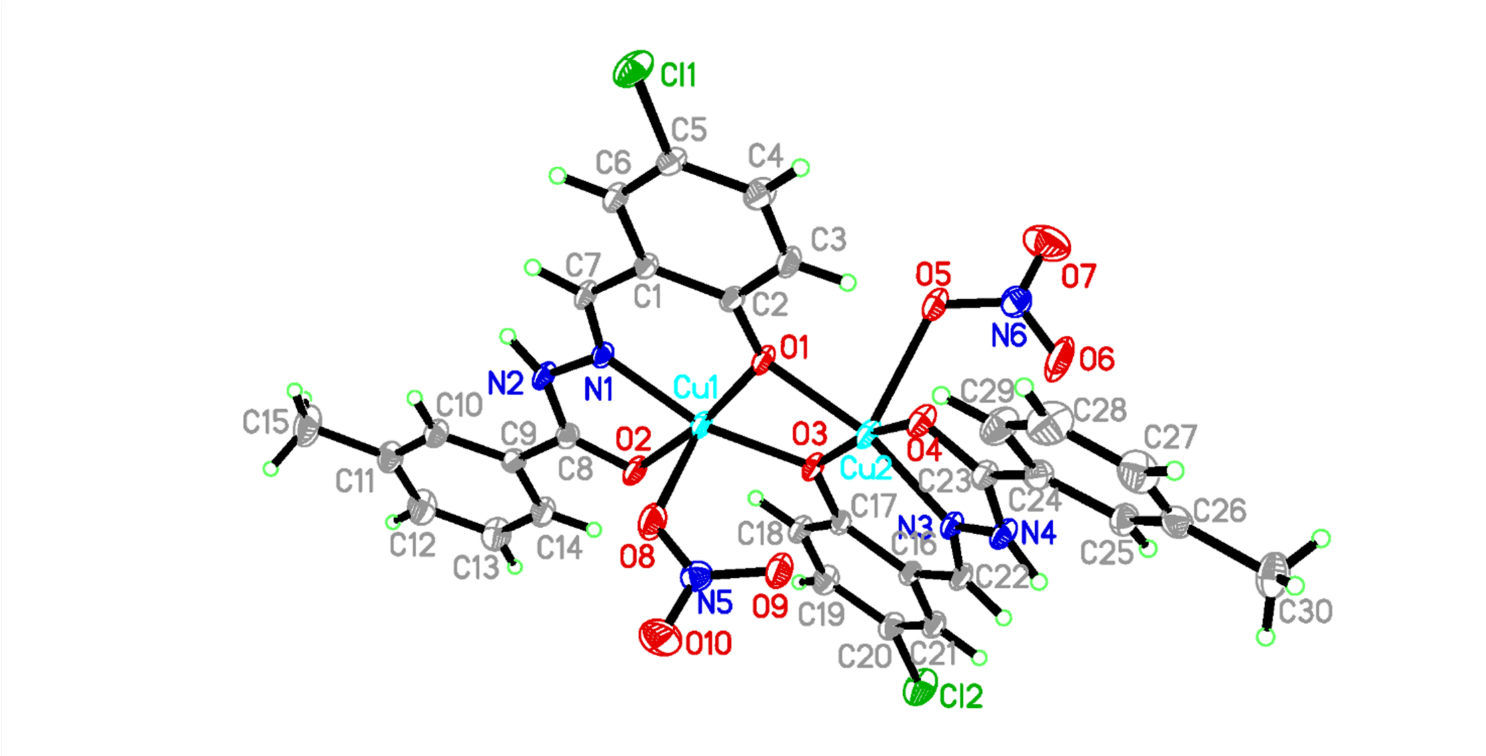

Figure 1

Molecular structure of complex **1**. Displacement ellipsoids for non-hydrogen atoms are drawn at the 30% probability level.

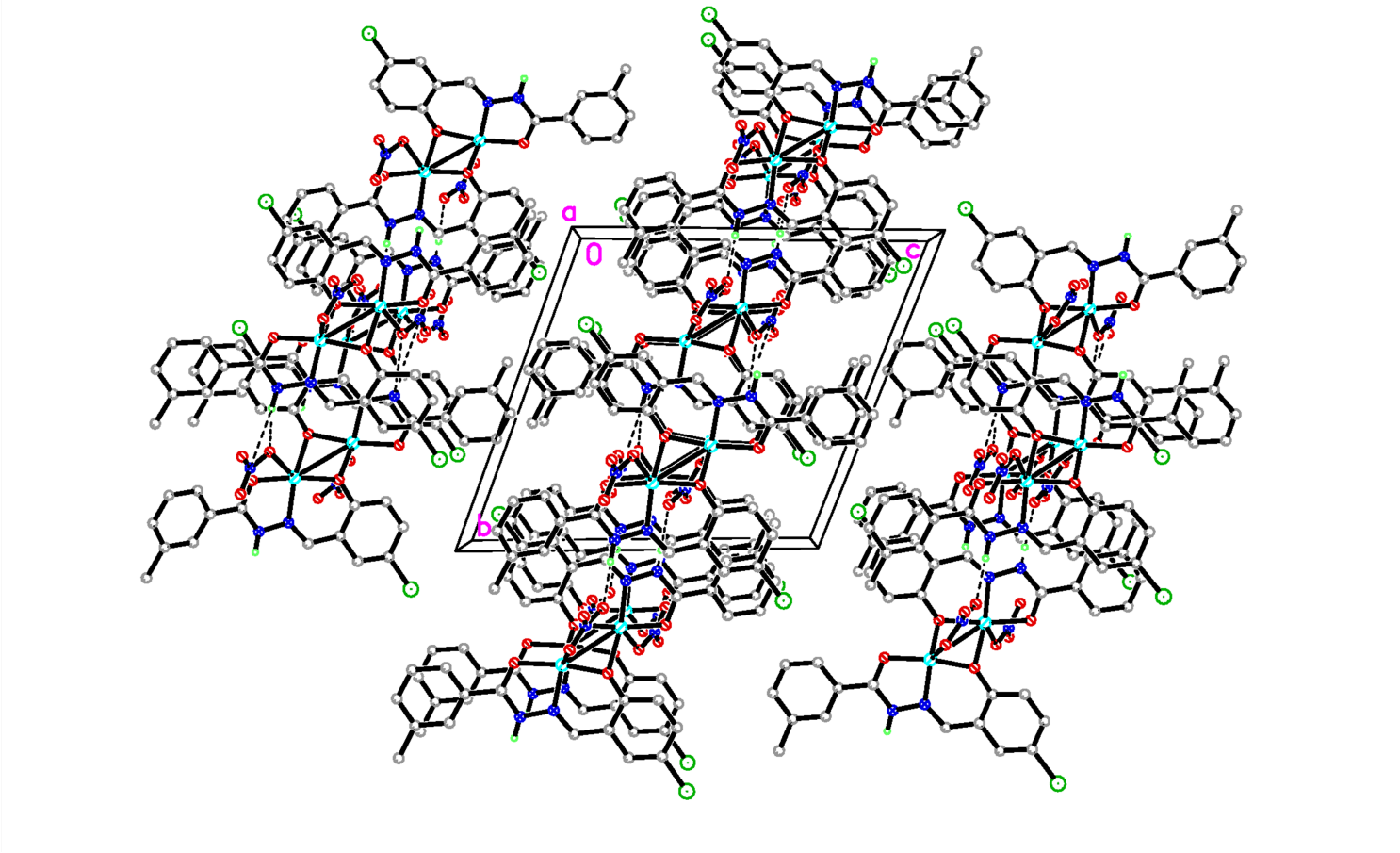

Figure 2

Molecular packing structure of complex **1**, viewed along *a* axis. Hydrogen bonds are shown as dashed lines.

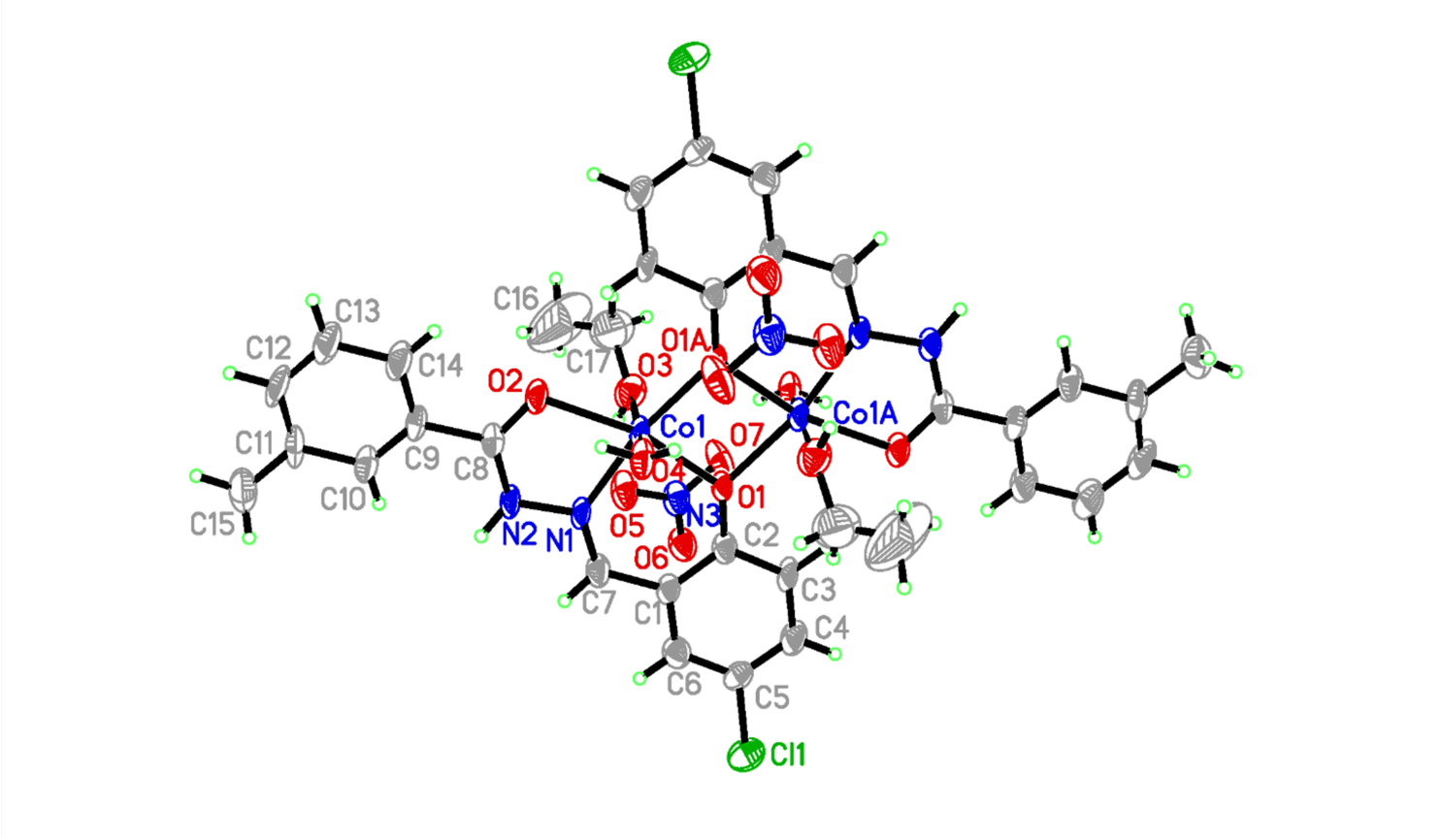

Figure 3

Molecular structure of complex **2**. Displacement ellipsoids for non-hydrogen atoms are drawn at the 30% probability level. Symmetry related atoms are related to the operation 1 – *x*, 2 – *y*, 1 – *z*.

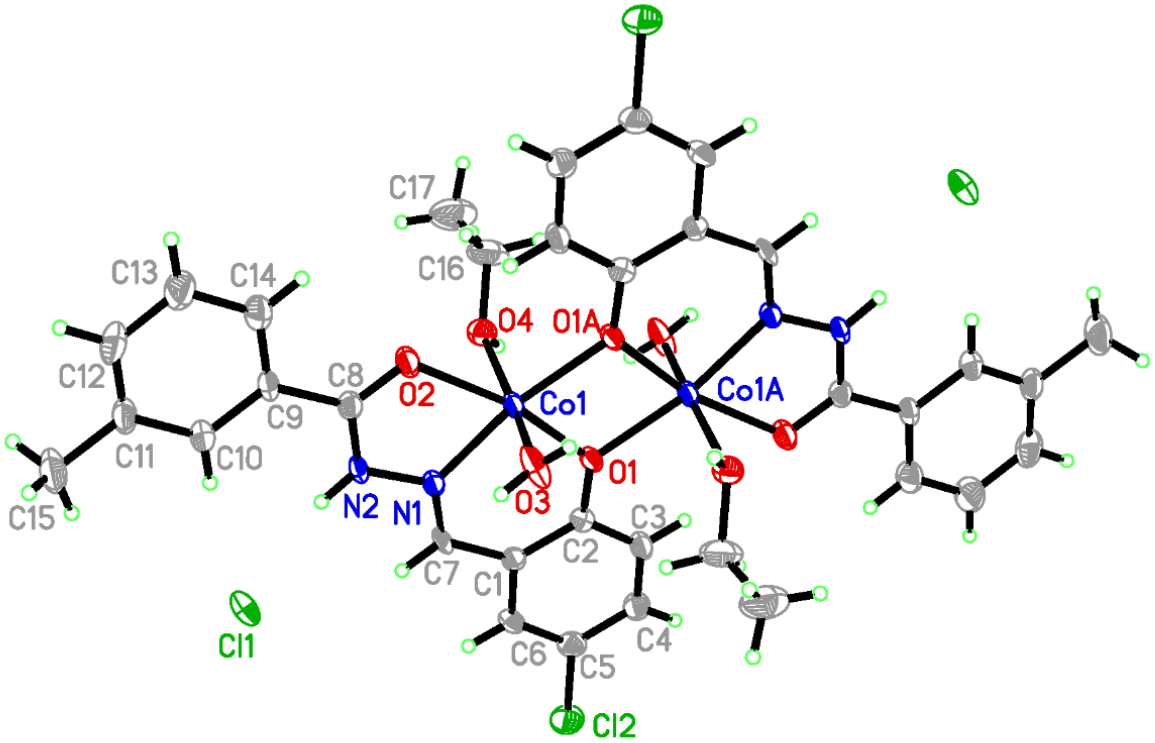

Figure 4

Molecular structure of complex **3**. Displacement ellipsoids for non-hydrogen atoms are drawn at the 30% probability level. Symmetry related atoms are related to the operation 1 − *x*, 2 − *y*, 1 − *z*.

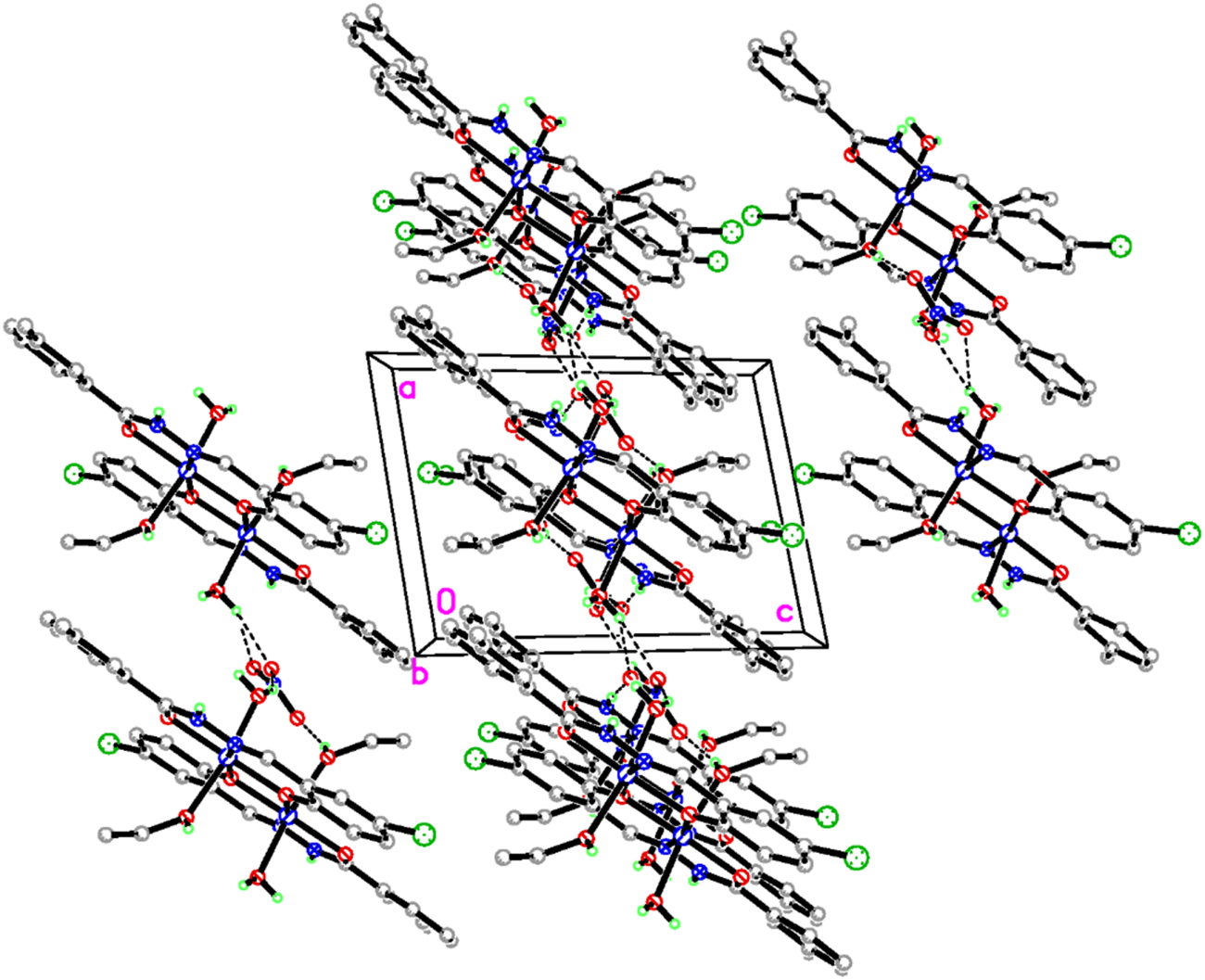

Figure 5

Molecular packing structure of complex **2**, viewed along *b* axis. Hydrogen bonds are shown as dashed lines.

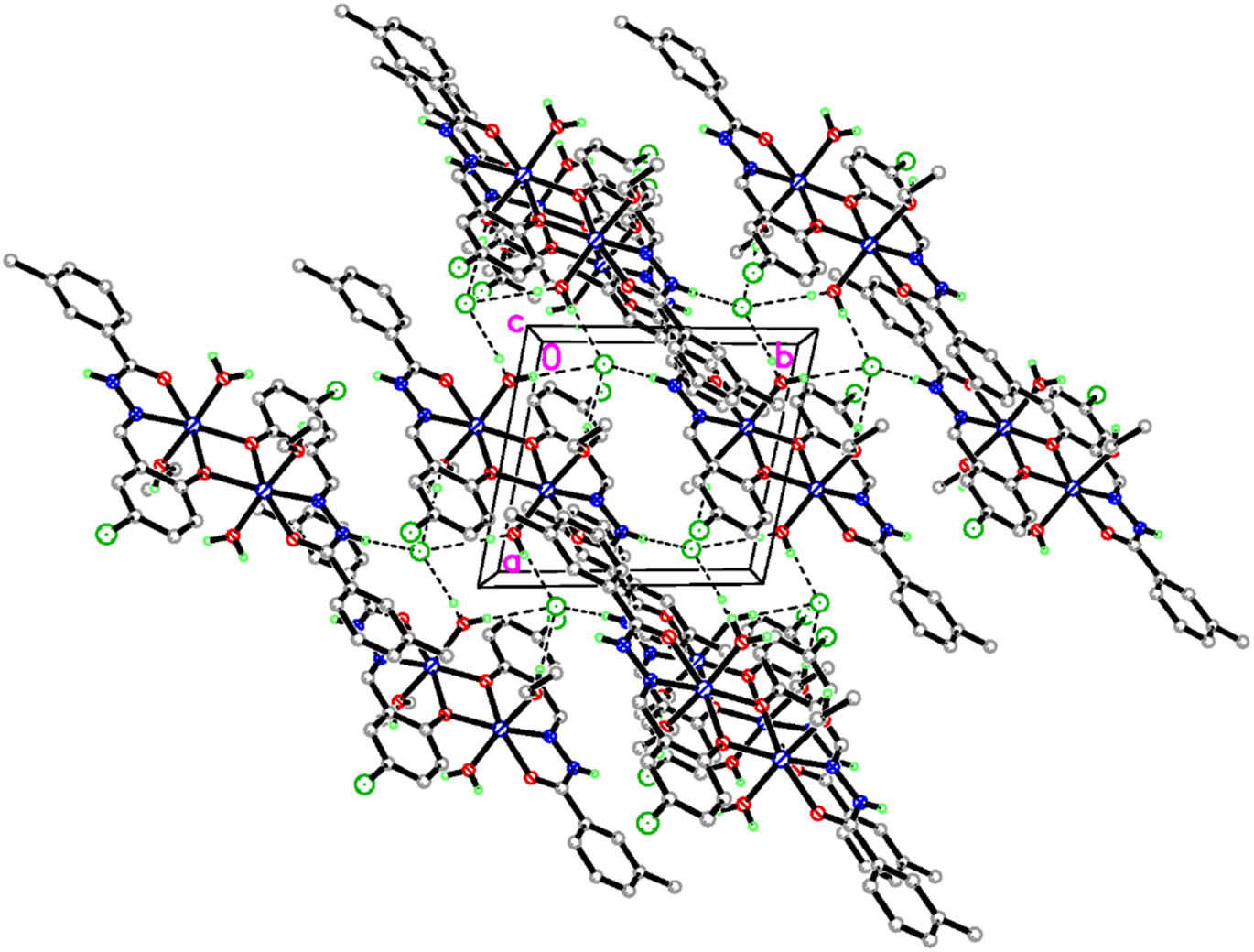

Figure 6

Molecular packing structure of complex **3**, viewed along *c* axis. Hydrogen bonds are shown as dashed lines.

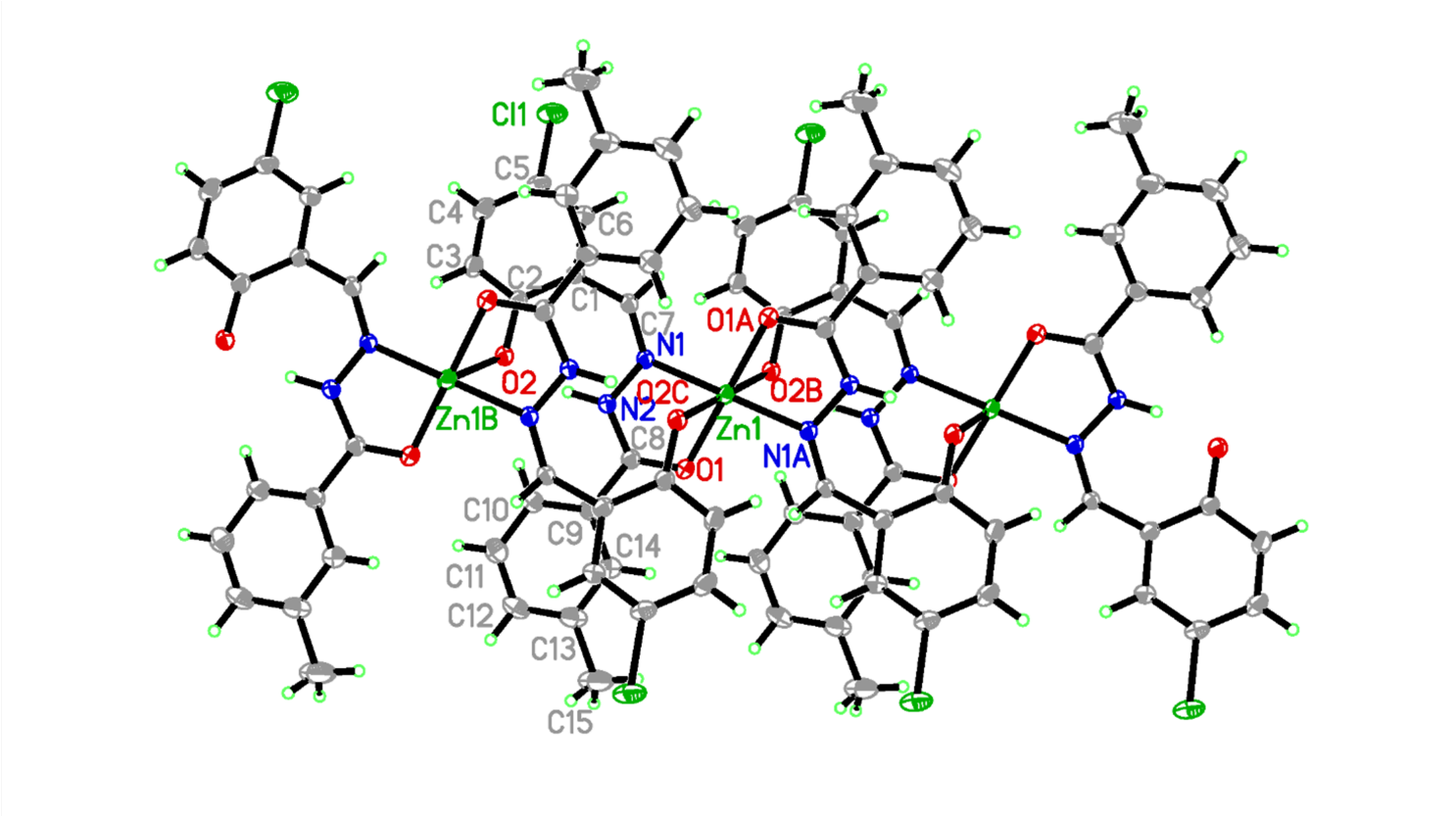

Figure 7

Molecular structure of complex **4**. Displacement ellipsoids for non-hydrogen atoms are drawn at the 30% probability level. Symmetry related atoms are related to the operations: A: 1 − *x*, 2 − *y*, 1 − *z*; B: *x*, 1 + *y*, *z*; C: 1 − *x*, 1 − *y*, 1 − *z*.

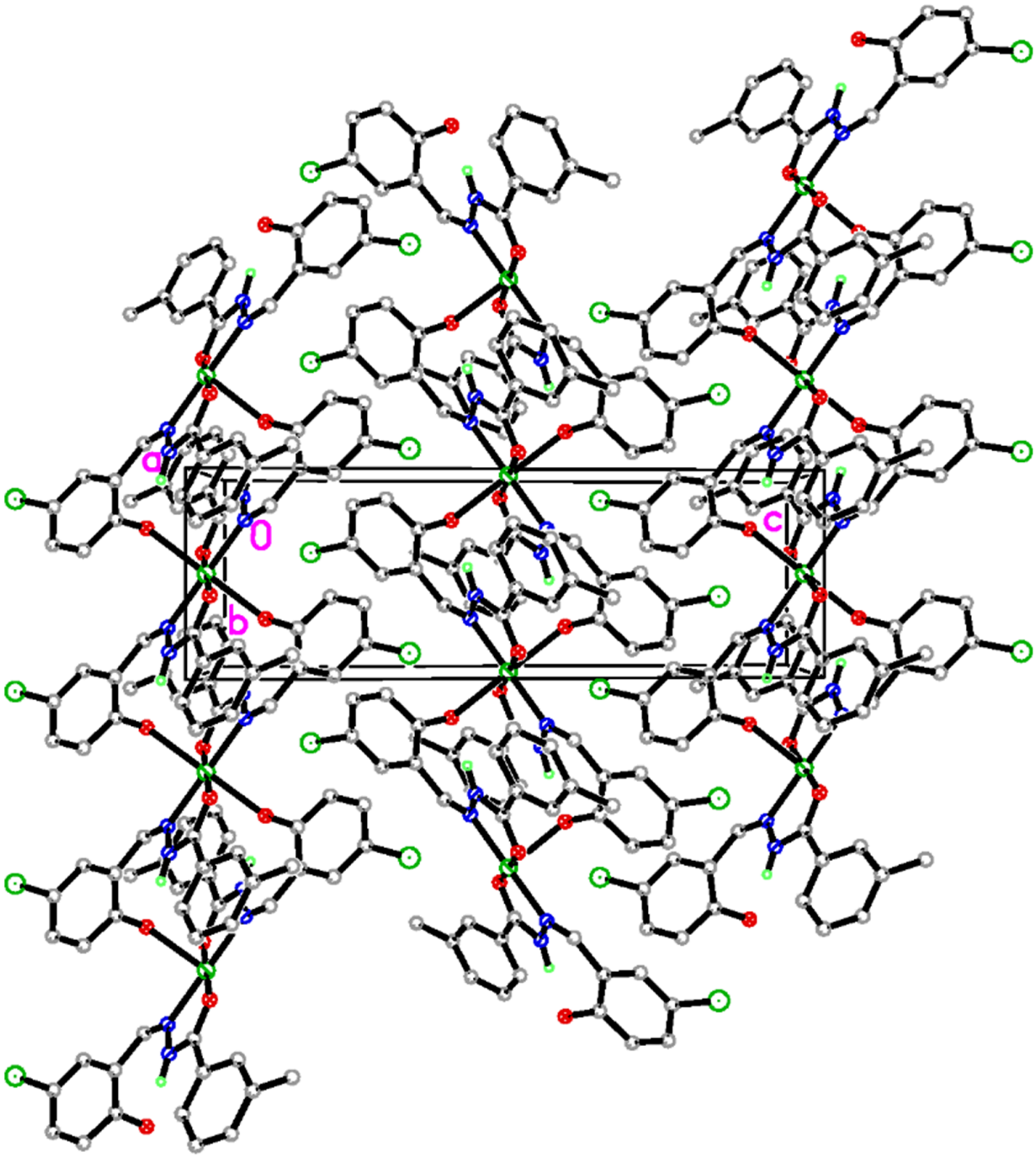

Figure 8

Molecular packing structure of complex **4**, viewed along *a* axis. Hydrogen bonds are shown as dashed lines.

Supplementary Files

This is a list of supplementary files associated with this preprint. Click to download.

- image1.png
- image2.png
- AppendixA.docx